

Measurements of Superoxide Anion Radical and Superoxide Anion Scavenging Activity by Electron Spin Resonance Spectroscopy Coupled with DMPO Spin Trapping

Masahiro KOHNO,* Yukio MIZUTA, Masako KUSAI, Toshiki MASUMIZU, and Keisuke MAKINO†
ESR Application Laboratory, Application and Research Center, Analytical Instruments Division, JEOL Ltd.,
1-2 Musashino 3 Chome, Akishima, Tokyo 196

† Kyoto Institute of Technology, Matsugasaki, Sakyo-ku, Kyoto 606

(Received August 26, 1993)

A quantitative analysis of superoxide anion radical ($\cdot\text{O}_2^-$) and hydroperoxyl radical ($\cdot\text{OOH}$) generated in the hypoxanthine–xanthine oxidase (HPX–XOD) reaction system in the presence of dimethyl sulfoxide (DMSO) was explored by a spin-trapping method using 5,5-dimethyl-1-pyrroline-*N*-oxide (DMPO) combined with electron spin resonance spectroscopy (ESR). $\cdot\text{O}_2^-$ and/or $\cdot\text{OOH}$ was detected by ESR spectra of the spin adduct, DMPO- O_2^- (or DMPO- OOH). The concentration of DMPO- O_2^- was increased up to three times by the addition of DMSO. The half-life of DMPO- O_2^- , which is the time period to reduce to one-half of the initial intensity, also became about 70 times longer than that in the system without DMSO. These results suggest that the short half-life of DMPO- O_2^- that has been reported is attributable to the partial reaction of hydroxyl radical ($\cdot\text{OH}$) with DMPO- O_2^- . Consequently quantitative analysis of $\cdot\text{O}_2^-$ was possible in the presence of DMSO (>0.35 M). Under these conditions, kinetic approaches show that the generation of $\cdot\text{O}_2^-$ in the HPX–XOD reaction is a first-order reaction and that its rate constant is $6.9 \times 10^{-8} \text{ Ms}^{-1}$. Finally, the competitive reaction of DMPO and SOD toward $\cdot\text{O}_2^-$ was shown to be one unit of superoxide dismutase (Cu/Zn–SOD) scavenging $\cdot\text{O}_2^-$ by the rate constant of $7.0 \times 10^{-6} \text{ M min}^{-1}$. This method, which can be used for measurement of SOD-like and SOD-mimic activity, should be called the superoxide anion scavenging activity method.

A blue copper protein called superoxide dismutase (Cu/Zn–SOD) was isolated for the first time from bovine erythrocytes by Mann and Keilin in 1939.¹⁾ In 1969, McCord and Fridovich reported that this protein was a catalyst for decomposition from superoxide anion radical ($\cdot\text{O}_2^-$) to hydrogen peroxide (H_2O_2) and molecular oxygen (O_2). And they also described the measurement of SOD activity and a method for measurement of $\cdot\text{O}_2^-$ in which various kinds of colorimetric reagents are used.²⁾ Several kinds of similar types of proteins have since been found by many research groups.^{3–5)}

The ESR-spin-trapping method has been used to detect $\cdot\text{O}_2^-$ in biological systems such as reperfused heart and bacterial endotoxin.^{6–9)} Also, SOD, SOD-like, and SOD-mimic activity of the biological materials has been measured by ESR based on the competitive reaction between such compounds and 5,5-dimethyl-1-pyrroline *N*-oxide (DMPO) for $\cdot\text{O}_2^-$.^{7–20)} Despite of these studies, it still remains difficult to do measurements by observing the spin adduct, DMPO- O_2^- , because of ready decomposition of DMPO- O_2^- to DMPO- OH and the reaction between DMPO- O_2^- and $\cdot\text{O}_2^-$.^{21–26)}

In this paper, we reinvestigated the hypoxanthine–xanthine oxidase (HPX–XOD) reaction in detail and discuss improved analysis of $\cdot\text{O}_2^-$ and the measurement of superoxide anion scavenging activity (SOSA). The activity unit of SOSA can be defined by use of the concentration of scavenged $\cdot\text{O}_2^-$ during one minute.

Experimental

Instruments. ESR measurements were done on a JEOL RE-1X ESR spectrometer connected with the computer systems, a JEOL-Espirit. *G* values and hyperfine

coupling constants (hfcc's) were calculated based on the resonance frequency measured with a microwave frequency counter and the resonance field measured with a field measurement unit, a JEOL-ES-FC5. Spin concentrations of the spin adducts of $\cdot\text{O}_2^-$, $\cdot\text{OH}$, and $\cdot\text{CH}_3$ were measured using 4-hydroxyl-2,2,6,6-tetramethylpiperidine-*N*-oxyl (TEMPOL) as a standard.

Preparation of Samples. $\cdot\text{O}_2^-$ was produced in the reaction system consisted of HPX and XOD. HPX and XOD (from cow's milk) were purchased from Sigma Chemical Co. (St. Louis, MO.) and Boehringer Mannheim GmbH (Mannheim, Germany), respectively. Highly purified DMPO was obtained from Dojin Laboratories (Kumamoto, Japan), and used without purification. Copper–Zinc SOD (Cu/Zn–SOD) from bovine and recombinant human Cu/Zn–SOD were obtained from Boehringer Mannheim GmbH and Nippon Kayaku Co., Ltd. (Tokyo). Activities of these Cu/Zn–SOD were measured by the cytochrome *c* method as described in according to the previous report,²⁾ and were 3130 units mg^{-1} and 4160 units mg^{-1} protein, respectively.

Reaction Conditions. One hundred mM (1 M = 1 mol dm^{-3}) sodium phosphate buffer solution with pH 7.8 was used as a solvent. A solution of 2.0 mM HPX (a) and 0.4 unit ml^{-1} XOD (b) were prepared to use at the next preparation step of the sample. Two kinds of sampling conditions were selected. One was that 50 μl of HPX, 185 μl of several dimethyl sulfoxide (DMSO) concentrations in water, and 15 μl of DMPO were put into a test tube. The other was that 50 μl of HPX, 285 μl of DMSO water solution, and 15 μl of DMPO were put into a test tube. After this, 50 μl of (b) was added to each solution. The total volume of the reaction solution was 300 or 400 μl . After it was stirred for 5 s, 130 μl of the mixed solution was taken into an aqueous flat ESR cell. After 30 s including mixing time, ESR spectra were recorded by a 30 s sweep or one minute sweep. Two reaction solutions were composed of 0.25 and 0.33 mM

of HPX, 0.35 and 0.46 M of DMPO, 0.042–0.055 unit/ml XOD, and 0–700 mM DMSO.

Results and Discussion

Assignment of Spin Adducts of Superoxide Anion Radical, Hydroxyl Radical, and Methyl Radical.

Figure 1 shows the ESR spectra of the spin adducts observed using DMPO (0.46 M) on the HPX (0.33 mM)–XOD (0.55 unit ml⁻¹) reaction systems. Figure 1a is the spectrum for the reaction system without DMSO. Figure 1b is for the reaction system containing 600 mM. The spectrum in Fig. 1a was constructed from the spectra of two type of spin adducts. Hfcc values for one of the spin adducts were analyzed as follows: $\alpha_N = 1.41$ mT, $\alpha_H^\beta = 1.14$ mT, and $\alpha_H^\gamma = 0.13$ mT. The hfcc's of the other spin adduct are $\alpha_N = 1.49$ mT and $\alpha_H^\beta = 1.49$ mT. Each component of the spectrum was assigned to DMPO–O₂⁻ (–OOH) and DMPO–OH, respectively, according to reported values.²⁷⁾ Upon the addition of DMSO, another spectrum appeared as shown in Fig. 1b. This signal increased with the dependence on the decreasing of that of DMPO–OH. The hfcc's of new signal are $a_N = 1.64$ mT and $\alpha_H^\beta = 2.24$ mT. These values coincide with the values reported for DMPO–CH₃.^{28,29)} The absolute concentrations of the spin adducts, DMPO–O₂⁻, obtained during one minute after preparation were measured by double integration by a computer system as 4.1×10^{-6} M for 600

mM DMSO and 2.1×10^{-6} M for 0 mM DMSO, respectively.

Stability of Spin Adduct, DMPO–O₂⁻. Figure 2 shows the profiles (scan interval being 5 s) of the formation of spin adducts, DMPO–O₂⁻ and DMPO–OH, in the reaction systems consisting of 0.25 mM HPX, 0.35 M DMPO, and 0.05 unit ml⁻¹ XOD. The profiles (a), (b), and (c) were obtained for the low field signals in Fig. 1b in the presence of 0, 175, and 300 mM DMSO, respectively. The signal intensity of DMPO–O₂⁻ are plotted against the reaction time for various concentration of DMSO (0–700 mM) as shown in Fig. 3a. Upon the addition of 700 mM DMSO, the intensity of DMPO–O₂⁻ signal was enhanced to about three times comparing with that without DMSO. At the maximum intensity region, the changing speed of signal intensity become slower. To discover the mechanism of the enhancement and the stabilization of this spin adduct, absolute concentration of DMPO–O₂⁻, DMPO–OH, and DMPO–CH₃ was calculated by using the ESR spectra observed during one minute after the start of the HPX–XOD reaction. The concentration of DMPO–O₂⁻ and DMPO–CH₃ observed upon the addition of 700 mM

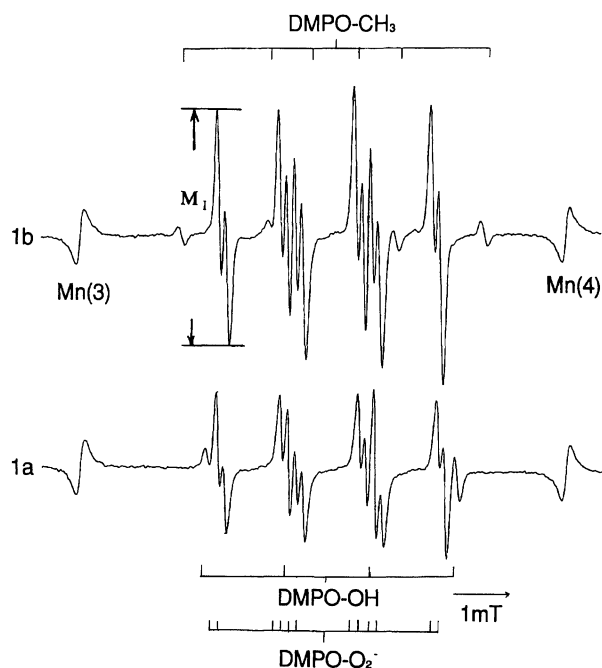


Fig. 1. ESR spectra of spin adducts observed using DMPO as a spin trap reagent in the HPX–XOD reaction. Spectrum 1a was observed under these conditions; 0.25 mM of HPX, 0.35 M of DMPO, 0.05 unit ml⁻¹ of XOD and 600 mM of DMSO. Spectrum 1b was observed under the same condition except DMSO.

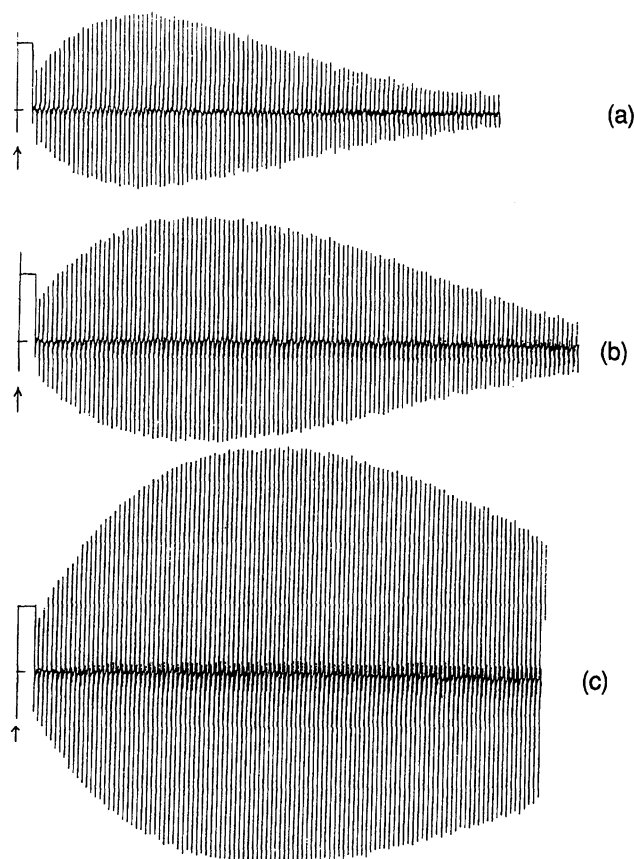


Fig. 2. Changes in DMPO–O₂⁻ and DMPO–OH signal intensities at lowest field ($M_1=1$) in Fig. 1b. The concentrations of DMSO in the reaction system are a) No DMSO, b) 175 mM DMSO, c) 300 mM DMSO. Acquisition interval is 5 s.

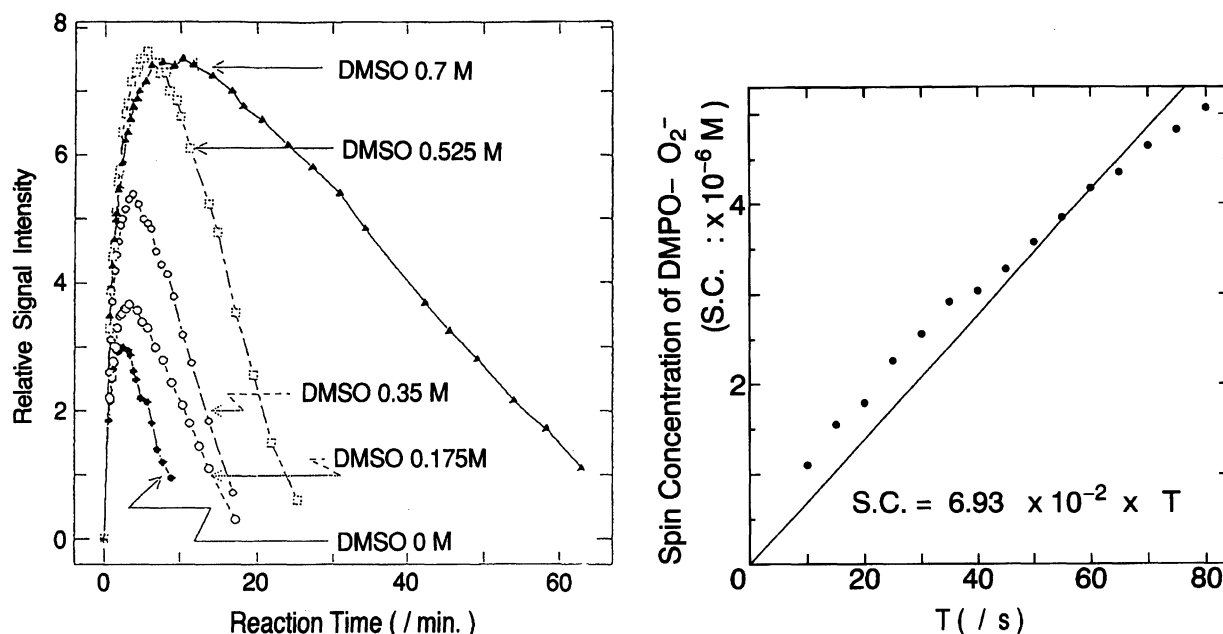
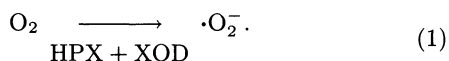


Fig. 3. a) Time dependence of the ESR signal intensities of DMPO-O₂⁻. The concentration of DMSO was varied; 0, 175, 350, 535, 700 mM. b) The plot of the ESR signal intensities of DMPO-O₂⁻ against the initial reaction times. Reaction conditions: 0.25 mM of HPX, 0.35 M of DMPO, 700 mM of DMSO, and 0.05 unit ml⁻¹ of XOD.

DMSO were 4.1×10^{-6} M and 1.9×10^{-7} M, respectively. The concentration of DMPO-CH₃ is nearly equal to that of DMPO-OH. These results suggest that DMSO reacts selectively with the hydroxyl radical ($\cdot\text{OH}$) and the equivalent amount of methyl radical ($\cdot\text{CH}_3$) was generated.²⁹⁾ These results show that the stability of DMPO-O₂⁻ was dependent on the concentration of $\cdot\text{OH}$, and that the life-time of DMPO-O₂⁻ was not related the reaction between $\cdot\text{O}_2^-$ and DMPO-O₂⁻. Therefore, it should be reevaluated to remove erroneous conclusions such as the reaction from DMPO-OOH to DMPO-OH in the biological systems.²⁴⁻²⁶⁾

Kinetics for the Generation of $\cdot\text{O}_2^-$. The reaction between HPX and XOD can be explained as



Assuming the concentration of $\cdot\text{O}_2^-$ is comparable to DMPO-O₂⁻,¹⁹⁾ the concentration of generated $\cdot\text{O}_2^-$ in the reaction system including 0.25 mM HPX, 0.35 M DMPO, 0.042 unit ml⁻¹ XOD, and 700 mM DMSO at 23 °C were obtained for each reaction time (Fig. 3b). From the figure, the $\cdot\text{O}_2^-$ generation from O₂ at the initial stage of the HPX-XOD reaction is first order, and the rate constant ($k_{\text{HPX-XOD}}$) was 6.9×10^{-8} M s⁻¹ (4.1×10^{-6} M min⁻¹). In addition, as is shown in Fig. 4, the Michaelis constant, K_m , and rate constant, V_{max} , were 8.3×10^{-6} M and 4.5×10^{-6} M min⁻¹ from a Lineweaver-Burk plot for various concentrations of HPX (0–128 mM), respectively. From the experimental results, V_{max} coincided with $k_{\text{HPX-XOD}}$.

Estimation of Produced H₂O₂ and $\cdot\text{OH}$ in the HPX-XOD Reaction System. The concentra-

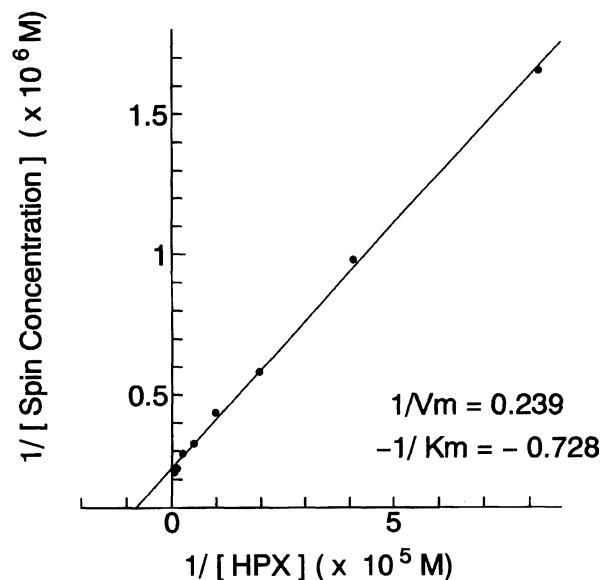
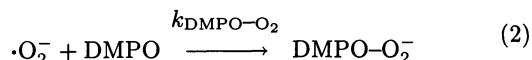


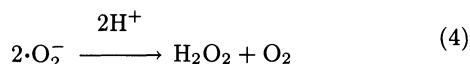
Fig. 4. Lineweaver-Burk plot for the HPX-XOD reaction.

tion of DMPO-O₂⁻ generated for one minute in addition of 700 mM DMSO was 4.1×10^{-6} M (6.9×10^{-8} M s⁻¹). The concentration of H₂O₂, and $\cdot\text{OH}$ was estimated using the concentration of DMPO-O₂⁻ by the kinetic approach. As already reported,¹⁹⁾ it is useful to consider the first step as the contact reaction between $\cdot\text{O}_2^-$ and DMPO. The rate constant ($k_{\text{DMPO-O}_2^-}$) between DMPO and $\cdot\text{O}_2^-$ was $16.9 \text{ M}^{-1} \text{ s}^{-1}$ as already reported.¹⁹⁾ Therefore, the concentration of $\cdot\text{O}_2^-$ produced in the reaction was estimated by the Eq. 3,



$$d[\text{DMPO-O}_2^-]/dt = k_{\text{DMPO-O}_2}[\text{DMPO}][\cdot\text{O}_2^-] \quad (3)$$

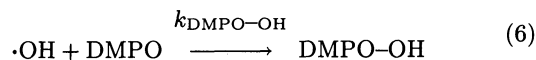
Since [DMPO] used in this experiments was 0.35 M, the absolute concentration of $\cdot\text{O}_2^-$, $[\cdot\text{O}_2^-]$, was calculated by the equation 3 to be 1.17×10^{-8} M. On the other hand, the rate constant for spontaneous dismutation between $\cdot\text{O}_2^-$ and $\cdot\text{O}_2^-$ at neutral pH is generally agreed to be $1.7 \times 10^7 \text{ M}^{-1} \text{ s}^{-1}$.³⁰⁾ The concentration of H_2O_2 was estimated using the rate constant by Eq. 5,



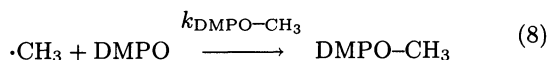
$$d[\text{H}_2\text{O}_2]/dt = k_{\text{H}_2\text{O}_2}[\cdot\text{O}_2^-][\cdot\text{O}_2^-] \quad (5)$$

As $[\cdot\text{O}_2^-]$ was already calculated as 1.17×10^{-8} M, $d[\text{H}_2\text{O}_2]/dt$ was calculated to be $2.3 \times 10^{-9} \text{ M s}^{-1}$.

In the experimental system with addition of DMSO, the reaction mechanism between $\cdot\text{OH}$ and DMSO can be described as



and



Assuming that the rate of formation of DMPO-CH₃ is comparable to that of DMPO-OH,

$$\begin{aligned} d[\text{DMPO-CH}_3]/dt &\approx d[\text{DMPO-OH}]/dt \\ &= k_{\text{DMPO-OH}}[\text{DMPO}][\cdot\text{OH}] \quad (9) \end{aligned}$$

The rate constant of DMPO-CH₃ generation in the HPX-XOD reaction can be estimated using the equation 9 to be $3.2 \times 10^{-9} \text{ M s}^{-1}$ from the concentration of DMPO-CH₃, which was observed during one minute after the reaction started. This concentration is connected with the estimated rate, $d[\text{H}_2\text{O}_2]/dt$, $2.3 \times 10^{-9} \text{ M s}^{-1}$. Therefore, the enhancement of DMPO-O₂⁻ was presumed to be from DMPO-O₂⁻ directly reacting with $\cdot\text{OH}$ and decaying by the oxidation or reduction actions.³¹⁾ From the calculation, main dismutation of $\cdot\text{O}_2^-$ can also be explained by the reaction between $\cdot\text{O}_2^-$ and $\cdot\text{O}_2^-$.

Calculation of DMSO Concentration Preferred to Stabilize DMPO-O₂⁻. DMSO concentration of perfectly scavenged $\cdot\text{OH}$ in this reaction system can be estimated theoretically using Eq. 10,

$$k_{\text{DMPO-OH}}[\text{DMPO}][\cdot\text{OH}] = k_{\text{DMSO-OH}}[\text{DMSO}][\cdot\text{OH}] \quad (10)$$

Although the second order rate constants of DMSO and DMPO for $\cdot\text{OH}$ have been reported as $6 \times 10^9 \text{ M}^{-1} \text{ s}^{-1}$ and $1.7\text{--}3.4 \times 10^9 \text{ M}^{-1} \text{ s}^{-1}$,³²⁻³⁴⁾ respectively, if $[\cdot\text{OH}]$ is constant and [DMPO] is 0.35 M, the minimum concentration of DMSO in order to scavenge 50% of $\cdot\text{OH}$

was estimated as 175 mM. The DMSO concentration (500 to 700 mM) used in this study was sufficient to stabilize DMSPO-O₂⁻, as shown in Fig. 3a. It is probable that the life-time of DMPO-O₂⁻ depends on the concentration of secondly generated $\cdot\text{OH}$ from H_2O_2 by the Haber-Waiss reaction.³⁵⁾

Definition of Activity of Superoxide Dismutase. The standard assay is done using 130 μl of 0.025 M potassium phosphate buffer (pH 7.8) in an aqueous flat ESR cell. Final concentration of DMPO and HPX were 0.35 M and 0.25 mM, respectively. When Cu/Zn-SOD of various concentrations (0.03—1.62 unit ml^{-1}) were added to the reaction system. ESR spectra of DMPO-O₂⁻ shown in Fig. 5 were obtained. In the figure, the ESR signal intensities of DMPO-O₂⁻ decreased with increases of the SOD concentration. These spectra show that the reaction between DMPO and $\cdot\text{O}_2^-$ was inhibited by the Cu/Zn-SOD. In Fig. 6, the DMPO-O₂⁻ intensities are plotted against the reaction time for various concentrations of SOD. Figure 7 shows the correlation between SOD activity and concentration of DMPO-O₂⁻ inhibited in 1 min. From the figure, the inhibition rate by the 1 unit of SOD was defined as $7.0 \times 10^{-6} \text{ M min}^{-1}$. This value coincided with the reported rate constants ($5 \times 10^{-6} \text{ M min}^{-1}$) which is de-

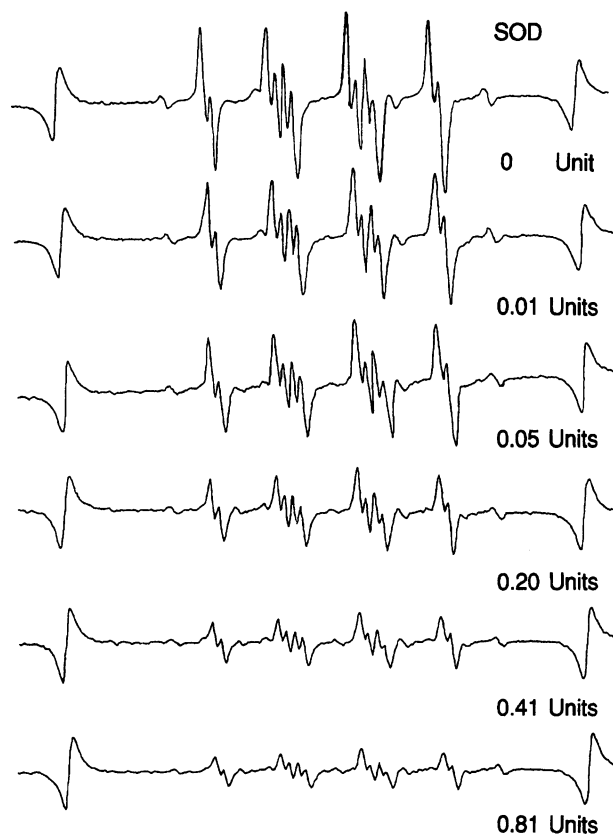


Fig. 5. ESR spectra of spin adducts produced in the HPX-XOD reaction. The reaction mixture contained 0.25 mM of HPX, 0.35 M of DMPO, 0.05 unit ml^{-1} of XOD and 0—0.81 unit ml^{-1} of SOD.

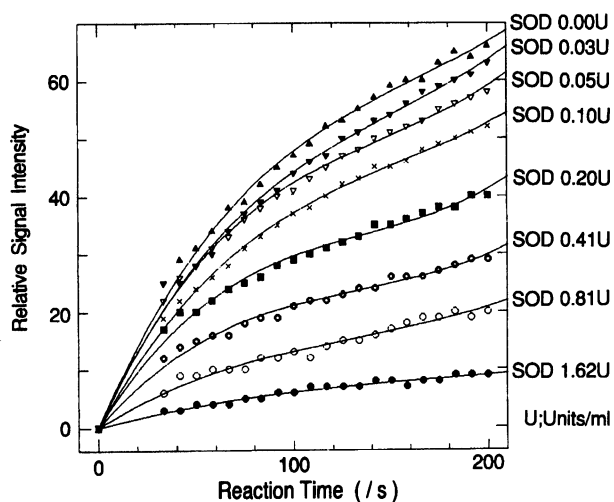


Fig. 6. The spin concentration of DMPO- O_2^- against the SOD concentration (0.003–1.62 unit ml^{-1}).

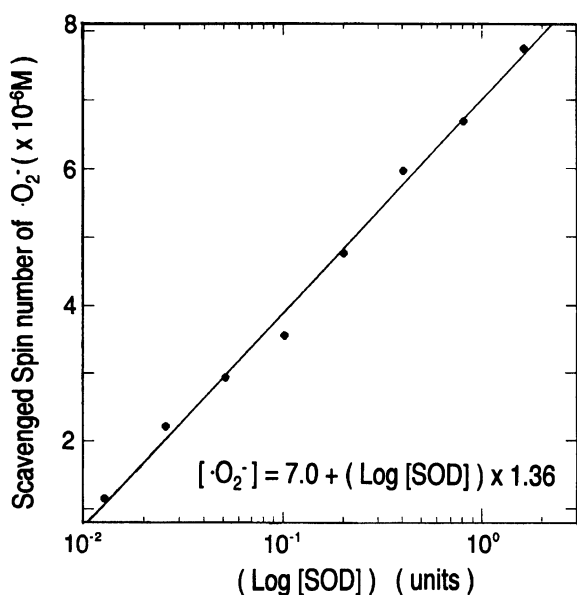


Fig. 7. Relationships between SOD activities and scavenged spin concentration of O_2^- .

finied by the cytochrome *c* method.²⁾

In conclusion, the ESR-spin-trapping method is more useful for measurement of SOD and SOD-mimic activity than the cytochrome *c* method because the ESR method provides direct observation of O_2^- inhibition profiles.

The following results were obtained for the HPX-XOD reaction by the ESR Spin-Trapping method. 1) Reliable measurements of O_2^- are attained by the addition of DMSO, which scavengers secondarily generated $\text{OH}\cdot$. 2) Overall reaction mechanisms were explained by the kinetic approaches. Finally, 3) The ESR spin-trapping method with DMPO will give new information for the quantitative analysis of O_2^- in biological systems.

References

- 1) T. Mann and D. Keilin, *Proc. R. Soc. London, Ser. B. Biol. Sci.*, **126**, 303 (1939).
- 2) J. M. McCord and I. Fridovich, *J. Biol. Chem.*, **244**, 6049 (1969).
- 3) B. B. Keele, J. M. McCord, and I. Fridovich, *Biol. Chem.*, **245**, 6176 (1970).
- 4) I. Fridovich, *Adv. Enzymol.*, **41**, 35 (1974).
- 5) F. J. Yost and I. Fridovich, *J. Biol. Chem.*, **248**, 4905 (1973).
- 6) C. M. Arroyo, J. H. Benjamin, B. F. Dickens, and W. B. Wegliki, *FEBS Lett.*, **221**, 101 (1987).
- 7) J. L. Zweier, *J. Biol. Chem.*, **263**, 1353 (1988).
- 8) S. K. Jackson, J. M. Stark, C. C. Rowlands, and J. C. Evans, *Free Radicals Med.*, **7**, 165 (1989).
- 9) J. Kajihara, M. Enomoto, K. Katoh, K. Mitsuta, and M. Kohno, *J. Biochem.*, **104**, 855 (1988).
- 10) E. Finkelstein, G. M. Rosen, E. J. Rauckman, and J. Paxton, *J. Mol. Pharmacol.*, **16**, 676 (1979).
- 11) I. Ueno, M. Kohno, K. Yoshihira, and I. Hirano, *J. Pharm. Dyn.*, **7**, 563 (1984).
- 12) I. Ueno, M. Kohno, K. Haraikawa, and I. Hirano, *J. Pharm. Dyn.*, **7**, 798 (1984).
- 13) H. Hiramatsu and M. Kohno, *JEOL News.*, **23A**, 7 (1987).
- 14) H. Miyagawa, T. Yoshikawa, T. Tanigawa, N. Yoshida, S. Sugino, M. Kondo, H. Nishikawa, and M. Kohno, *J. Clin. Biochem. Nutr.*, **5**, 1 (1988).
- 15) T. Hatano, R. Edamatsu, M. Hiramatsu, A. Mori, Y. Fujita, T. Yasuhara, T. Yoshida, and T. Okuda, *Chem. Pharm. Bull.*, **37**, 2016 (1989).
- 16) J. Jinno, H. Mori, Y. Oshiro, T. Kikuchi, and H. Sakurai, *Free Radicals Res. Commun.*, **15**, 223 (1991).
- 17) M. Hiramatsu, M. Kohno, R. Edamatsu, K. Mitsuta, and A. Mori, *J. Neurochem.*, **58**, 1160 (1992).
- 18) R. Ogura, H. Ueta, M. Sugiyama, B. P. Pharm, and T. Hidaka, *J. Invest. Dermatol.*, **94**, 227 (1990).
- 19) K. Mitsuta, Y. Mizuta, M. Kohno, M. Hiramatsu, and A. Mori, *Bull. Chem. Soc. Jpn.*, **63**, 187 (1990).
- 20) B. Gray and A. J. Carmichael, *Biochem. J.*, **281**, 795 (1992).
- 21) B. Kalyanaraman, C. C. Felix, and R. C. Sealy, *Photochem. Photobiol.*, **36**, 5 (1982).
- 22) G. R. Buettner, *Free Radicals Res. Commun.*, **10**, 11 (1990).
- 23) A. Samuni, C. Murali Krishna, P. Riese, E. Finkelstein, and A. Russo, *Free Radicals Mol.*, **6**, 141 (1989).
- 24) M. R. Green, H. Allen, O. Hill, M. J. Okolow-Zubkowska, and A. W. Segal, *FEBS Lett.*, **100**, 23 (1979).
- 25) B. E. Britigan, G. M. Rosen, Y. Chai, and M. S. Cohen, *J. Biol. Chem.*, **261**, 4426 (1986).
- 26) I. Ueno, M. Kohno, K. Mitsuta, Y. Mizuta, and S. Kanegasaki, *J. Biochem.*, **105**, 905 (1989).
- 27) J. R. Harbour, V. Chow, and J. R. Bolton, *Can. J. Chem.*, **52**, 3549 (1974).
- 28) G. R. Buettner, *Free Radicals Biol. Med.*, **3**, 259 (1987).
- 29) M. Kohno, M. Yamada, K. Mitsuta, Y. Mizuta, and T. Yoshikawa, *Bull. Chem. Soc. Jpn.*, **64**, 1447 (1991).

- 30) G. H. Czapski and L. M. Dorfman, *J. Phys. Chem.*, **68**, 1169 (1964).
31) P. Kuppusamy and J. L. Zweier, *J. Biol. Chem.*, **15**, 9880 (1989).
32) M. G. Simic, *Mutat. Res.*, **202**, 377 (1988).
33) T. Tanigawa, *J. Kyoto Pref. Univ. Med.*, **99**, 133 (1990).
34) E. Finkelstein, G. M. Rosen, E. J. Rauckman, and J. Paxton, *J. Mol. Pharmacol.*, **16**, 676 (1979).
35) F. Haber and J. Weiss, *Naturwissenschaften*, **20**, 948 (1932).
-